Available online at www.sciencedirect.com
ScienceDirect
Journal of Nuclear Materials 367–370 (2007) 160–165
journal of nuclear materials
www.elsevier.com/locate/jnucmat

Nano-mesoscopic structural characterization of 9Cr-ODS martensitic steel for improving creep strength

S. Ohtsuka *, S. Ukai [1], H. Sakasegawa, M. Fujiwara, T. Kaito, T. Narita

Advanced Nuclear System R&D Directorate, Japan Atomic Energy Agency, 4002, Narita, Oarai, Ibaraki 311-1393, Japan

Abstract

This paper describes the effect on creep strength and microstructure of 9Cr-oxide dispersion strengthened martensitic steel (9Cr-ODS steel) produced by differences in titanium concentration and consolidation temperature. The increase of titanium concentration to 0.30–0.35 wt% was shown to provide considerable improvement of creep strength accompanied by the increase of residual-α ferrite. The elevation of hot-extrusion temperature degraded the creep strength, however, it appeared to increase the volume fraction of residual-α ferrite. The creep deformation process of 9Cr-ODS steel was discussed to explain these results based on microstructure observations.
© 2007 Elsevier B.V. All rights reserved.

1. Introduction

Development of advanced materials resistant to high-temperature and the radiation environment are essential for a fusion reactor system to achieve adequate economical performance. Oxide-dispersion-strengthened (ODS) martensitic steel has a swelling-resistant matrix with the capacity for trapping point defects [1], in which small oxide particles are dispersed to improve high-temperature strength. Japan Atomic Energy Agency (JAEA) has developed the 9Cr-ODS martensitic steel (9Cr-ODS steel) for fast reactor applications and has succeeded in manufacturing the thin-walled tubes that overcome the strength anisotropy [2,3]. This paper describes the effect on microstructure and creep strength of the 9Cr-ODS steel produced by differences in titanium concentration and consolidation temperature.

2. Experimental procedure

2.1. Materials

Table 1 shows the chemical analysis results of the 9Cr-ODS steels used in this study, where excess oxygen concentration is defined as the value obtained by subtracting oxygen concentration in Y_2O_3 from total oxygen concentration in the steel. Oxygen concentration was analyzed by means of inert gas fusion method. Titanium concentrations were controlled to either 0.2 wt%, 0.30 wt% or 0.35 wt%, and the excess oxygen concentrations from 0.026 wt% to 0.15 wt%. Designation of these steels

* Corresponding author. Tel.: +81 29 267 4141x6823; fax: +81 29 267 7173.
E-mail address: ohtsuka.satoshi@jaea.go.jp (S. Ohtsuka).
[1] Present address: Department of Materials Science and Engineering, Hokkaido University, N13, W8, Kita-ku, Sapporo 060-8628, Japan.

0022-3115/$ - see front matter © 2007 Elsevier B.V. All rights reserved.
doi:10.1016/j.jnucmat.2007.03.004

Table 1
Chemical analysis results (wt%) of 9Cr-ODS steels. Hot-extrusion temperature (T_e) is 1200 °C for 35MH and 1150 °C, for the rest

	35MS, 35MH	3MS	2HS	2MS	2LS	46MS
C	0.14	0.15	0.13	0.13	0.13	0.13
Cr	9.0	9.1	8.8	8.9	8.9	8.7
W	2.0	2.0	1.9	2.0	1.9	1.9
Ti	0.35	0.30	0.21	0.21	0.20	0.46
Y	0.28	0.28	0.27	0.28	0.27	0.27
O	0.16	0.18	0.22	0.16	0.099	0.18
Y_2O_3[a]	0.36	0.36	0.34	0.36	0.34	0.34
Ex.O[b]	0.084	0.10	0.15	0.084	0.03	0.11
σ_c[c]	198, 173	202	80	130	100	148
Hv(F)[d]	380, 390	–	(No ferrite)	–	–	–
Hv(M)[e]	350, 330	–	307	–	–	–

[a] Estimated from yttrium content with the assumption that yttrium exists as Y_2O_3.
[b] Defined as the value obtained by subtracting oxygen conc. in Y_2O_3 from the total oxygen conc. in steel.
[c] One thousand hour creep rupture strength at 700 °C (MPa).
[d] Average hardness of elongated grain (Hv).
[e] Average hardness of equiaxed grain (Hv).

is shown in Table 1, selected to indicate titanium concentration, oxygen concentration, either low (L), moderate (M) or high (H), and hot-extrusion temperature, either standard (S) or high (H), e.g. the designation 35MS indicates 0.35 wt% titanium, moderate concentration of oxygen and hot-extrusion at standard temperature (1150 °C). The rods made of 9Cr-ODS steel were manufactured through the general process described in previous reports [2]: mechanical alloying (MA) in argon-gas atmosphere and consolidation of mechanically-alloyed powders by hot-extrusion. The hot-extrusion temperature was 1200 °C for 35MH and 1150 °C for the rest.

2.2. Properties evaluation

Uni-axial creep tests of the 9Cr-ODS steels were carried out at 700 °C after normalizing-and-tempering (1050 °C × 1 h, air-cooling (AC) ⇒ 800 °C × 1 h, AC). The specimen gauge size was 6 mm in diameter and 30 mm in length. The stress loading in the creep tests was parallel to the extrusion direction. A procedure for showing the ferrite distribution is to observe where ferrite-forming elements preferentially partition during the heat treatment of 1050 °C × 1 h [4]. Through air-cooling subsequent to 1050 °C × 1 h annealing in the normalizing-and-tempering, austenite transforms into martensite while ferrite remains untransformed. Thus, electron probe microanalysis (EPMA) mapping of ferrite-forming elements that can estimate the distribution of ferrite and austenite at 1050 °C could be a promising technique for assessment of ferrite distribution in the martensite matrix. Tungsten (ferrite-forming element) was analyzed using an EPMA for estimating the fraction of residual α-ferrite [5,6] which remains untransformed during the consolidation process at high temperature. The EPMA analyzes were carried out after heat treatment of 1150 °C × 1h followed by water-quenching, where a rapid-cooling by quenching was adopted for reduction of carbide that contains tungsten. Oxide particles were characterized using a field-emission type transmission electron microscope (FE-TEM) after 1050 °C × 1 h heat treatment followed by a furnace-cooling at 30 °C/h to anneal dislocation microstructure and clearly show small oxide particles. Small angle scattering (SANS) study by Alinger et al. [7] showed that in 14Cr-ODS steel MA957, 1150 °C annealing for times up to 243 h has little effect on coarsening of dispersoids that contain yttrium, titanium and oxygen as in the 9Cr-ODS steel. This report encourages the authors to consider that oxide particle dispersion of the furnace-cooled 9Cr-ODS steel could agree with that of normalized-and-tempered steel without coarsening. Vickers microhardness measurements were carried out at 49 measurement points for a specimen after the normalizing-and-tempering (1050 °C × 1 h, AC ⇒ 800 °C × 1 h, AC). The measured points were arrayed in a square lattice (seven rows of seven points) with a separation distance of 25 μm. The size of the indent was ~5 μm. The workability of the 9Cr-ODS steel containing 0.3 wt% titanium (3MS) was examined by sending the steel through the tube manufacturing process [2]. The extruded bar of 3MS was mechanically worked into a mother tube with the dimension of 18 mm in diameter × 3 mm in wall-thickness and finished by furnace-cooling at 100–150 °C/h subsequent to 1050 °C × 1 h heat treatment. The tube manufacturing process consisted of four pass of cold-rolling with a pilger-mill followed by furnace-cooling at 100–150 °C/h subsequent to 1050 °C × 1 h heat treatment for softening. Vickers hardness of the steel was measured with 1 kgf loading after each step of the cold-rolling and the heat treatment.

3. Results and discussion

3.1. Creep strength

In terms of manufacturability to thin-walled tube that overcomes strength anisotropy, 9Cr-ODS

martensitic steels are thought to have the advantage over ODS ferritic steels (e.g. 12Cr-ODS steel developed by JAEA [3] and 12YWT [8]). Cold-rolling elongates the crystal grains along the rolling direction. In the case of ODS martensitic steels, the ferrite (α) to austenite (γ) reverse transformation provided by austenitization heat treatment allows the elongated grains to become adequately equiaxed. Furthermore, the austenite (γ) to ferrite (α) transformation, which is given by the austenitization followed by slow-cooling process, permits the work-hardening due to the cold-rolling to recover to a satisfactory level [2]. In the case of ODS ferritic steels, the matrix does not produce any reversible transformations such as the ferrite(α)/austenite(γ) transformation that allow the rolled-matrix to become equiaxed and adequately relieve its internal stress. This nature often causes the cold-rolled ODS ferritic steels to have a strength anisotropy – strength improvement in the rolling direction and deterioration in hoop direction – even after some heat treatments. A suitable procedure to overcome this anisotropy is recrystallization [3,9]. However, a careful choice of the reduction in cold-rolling and the annealing temperature is required for the control of that effect [3]. A weak point of 9Cr-ODS steel is its inferior creep strength caused by a fine grained microstructure. The creep rupture test results of 9Cr-ODS steel are presented in Fig. 1 as a function of Larson–Miller-Parameter (LMP) with a constant of 25, where creep data of unrecrystallized 12Cr-ODS ferritic steel (12YWT) [8], European 9Cr-ODS steel (ODS-EUROFER) [10] and 11Cr-martensitic steel (PNC-FMS [11]) were plotted for comparison. It is seen in the 9Cr-ODS steels containing 0.2 wt% titanium (2HS, 2MS, 2LS) that the moderate concentration of excess oxygen improves creep strength. This would be because the residual-α ferrite that strengthens the 9Cr-ODS steel remains in matrix when excess oxygen concentration is moderate as discussed in previous reports [5,6]. The creep tests of 12YWT were carried out with the load parallel to working direction – the high-strength direction [8]. It should be noted that creep strength of the 9Cr-ODS steel is considerably improved by increasing titanium concentrations from 0.2 wt% to either 0.3 wt% or 0.35 wt% (35MS, 35MH), thus reaching a level comparable to that of 12YWT. It is seen in Fig. 2 that creep strength is highest when titanium concentration is 0.30–0.35 wt%. The comparison of 35MS and 35MH reveals that elevation of hot-extrusion temperature from 1150 °C to 1200 °C deteriorates the creep strength. The 1000 h creep rupture strength at 700 °C shown in Fig. 2 was estimated from the LMP plot (Fig. 1) .

3.2. Microstructures and Vickers hardness

Microstructure characterization was carried out to understand the reason why the creep strength of 9Cr-ODS steel sensitively depends on titanium concentration and hot-extrusion temperature. In order to examine the effect of hot-extrusion temperature on the fraction of residual-α ferrite, the distributions of tungsten were evaluated as presented in

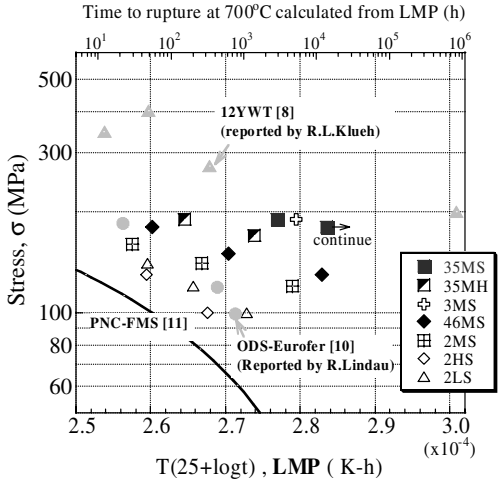

Fig. 1. Creep rupture strength of the 9Cr-ODS steels after normalizing-and-tempering (1050 °C × 1 h, AC ⇒ 800 °C × 1 h, AC).

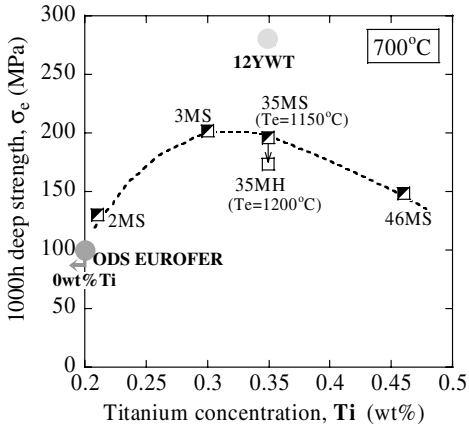

Fig. 2. One thousand hour creep rupture strength at 700 °C of the normalized-and-tempered 9Cr-ODS steels as a function of titanium concentration.

Fig. 3, which reveals that the elongated area parallel to extrusion direction where tungsten is concentrated is present in the high strength steels – 35MS and 35MH. The elongated area is considered to be residual-α ferrite which improves creep strength of the 9Cr-ODS steel. Tungsten is a ferrite-forming element having a higher partitioning ratio into ferrite compared with austenite, thereby preferentially partitioning into ferrite [4]. The improvement of creep strength in 35MS, 35MH would be attributed to the presence of residual-α ferrite in these steels. The elevation of hot-extrusion temperature appears to provide for the expansion of residual-α ferrite as seen in Fig. 3, although deteriorating the creep strength. This correlation between hot-extrusion temperature and fraction of residual-α ferrite is consistent with the phase-diagram for a chemical composition of 9 wt%Cr–0.13C–2W–0.35Y_2O_3–xTi (x: variable), which indicates the increase of ferrite with elevating temperature from 1150 °C to 1200 °C [6]. TEM observation results of 35MS and 35MH are presented in Fig. 4, which shows that oxide particles are more densely dispersed in the elongated grain – residual-α ferrite – than in the equiaxed grain – tempered martensite. No obvious difference can be seen in the size of dispersed oxide particles between 35MS and 35MH. With the intension of finding a clue to the understanding of the reason why the creep strength is degraded by elevating the hot-extrusion temperature, Vickers microhardness tests were performed after the normalizing-and-tempering. The hardened area was seen to elongate parallel to the hot-extrusion direction in 35MS and 35MH, while the hardness in 2HS was at a lower level and uniformly distributed. The elongated hardened area and the soft area should respectively correspond to residual-α ferrite and tempered martensite, considering the TEM observation result showing the finer oxide particle dispersion in residual-α ferrite than in tempered martensite (Fig. 4). The hardness of this elongated area in 35MS and 35MH is at the same level: Hv370–Hv410, while that of the soft area is higher in 35MS (350Hv) than in 35MH (330Hv). It may be said from these results that the elevation of hot-extrusion temperature should cause the tempered martensite phase – soft area – to be weakened probably due to the coarsening of oxide particles, thus deteriorating the creep strength. The limitation

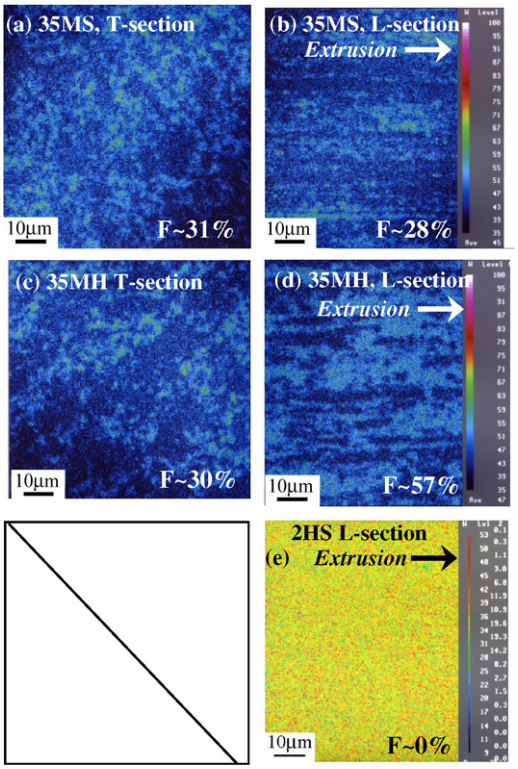

Fig. 3. EPMA mapping results of the tungsten distributions in 9Cr-ODS steels after water-quenching (WQ: 1150 °C × 1 h, water-quenching). (a) Transverse (T) section of 35MS (0.35 wt%Ti, hot-extrusion temperature (T_e) = 1150 °C), (b) Longitudinal (L) section of 35MS, (c) T-section of 35MH (0.35 wt%Ti, T_e = 1200 °C), (d) L-section of 35MH, (d) L-section of 2HS (0.2 wt%Ti, T_e = 1150 °C). The symbol F represents the area fraction of W-concentrated region.

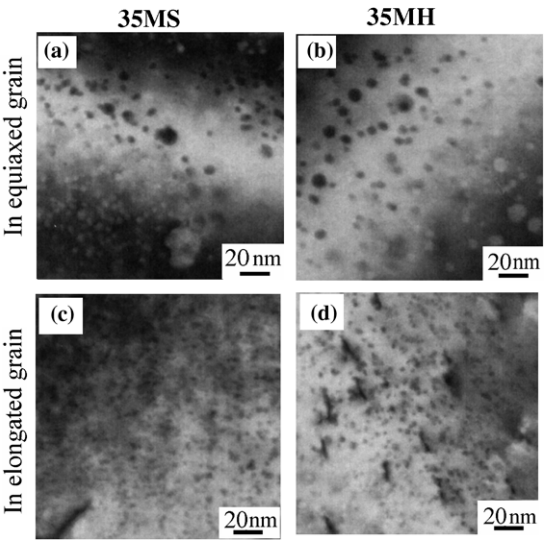

Fig. 4. TEM observation results of dispersed oxide particles in the furnace-cooled 9Cr-ODS steels: (a) in equiaxed grain of 35MS (T_e = 1150 °C, 0.35 wt%Ti, 0.08 wt%Ex.O), (b) in equiaxed grain of 35MH (T_e = 1200 °C, 0.35 wt%Ti, 0.08 wt%Ex.O), (c) in elongated grain of 35MS, and (d) in elongated grain of 35MH.

in the observed area by TEM might cause a considerable margin of error in the evaluation of oxide particle size in Fig. 4, which shows no obvious difference in the size of dispersed oxide particles between 35MS and 35MH. In addition, the nano-sized particles smaller than observable level of TEM might exert an influence on the hardness of 9Cr-ODS steel.

3.3. A possible model to explain the effects of titanium concentration and hot-extrusion temperature

The creep strength of 9Cr-ODS steel is certainly improved when the microstructure consists of hard grains-residual-α ferrite – and soft grains – tempered martensite (35MS, 35MH) compared to the specimen with uniform microstructure consisting of soft grains (2HS). The presence of hard grains eases the effective stress loading on the soft grains, since the hard grains support higher stress level in the same manner as in composite materials.

It was reported that threshold stress at 700 °C for deformation of 9Cr-ODS steel was estimated to be 323–494 MPa from TEM micrograph [2], while creep deformation at 700 °C occurs at a lower stress level than the threshold stress. This fact leads to consideration that creep deformation of 9Cr-ODS steel at 700 °C is enhanced by mechanisms other than dislocation-glide, e.g. grain boundary sliding and diffusion creep. On the other hand, considerable anisotropy in creep strength is seen at 700 °C in 12Cr-ODS ferritic steel that has anisotropic crystal grains with approximately a few tens of micrometers in length and several micrometers in diameter [3]. The presence of this strength anisotropy indicates that the deformation ascribed to fine grain size – i.e. grain boundary sliding and grain boundary diffusion creep – certainly occurs in the 12Cr-ODS steel. The grain size of 9Cr-ODS steel is less than a few micrometer [2], so that the creep deformation of 9Cr-ODS at 700 °C is enhanced by the fine grain size as in the 12Cr-ODS steel tested in the short axis direction of crystal grain. The stress exponent of steady state creep rate is believed to be 1–2 for grain boundary sliding as well as for grain boundary diffusion creep, while it is 3–7 for dislocation creep. The value for the 9Cr-ODS steel experimentally determined was 7–11 at 700 °C [12] that is a little higher but approximately agrees with the value for dislocation creep model. The grain boundary sliding would often be accompanied by other deformation process that accommodates the discontinuity produced by grain boundary sliding between neighboring grains. Considering the stress exponent and the fine grain size of 9Cr-ODS, grain boundary sliding accompanied by dislocation creep could be a primary creep mechanism for 9Cr-ODS steel at 700 °C. Dislocation creep that accommodates the discontinuity could be a rate limiting factor for grain boundary sliding. It is noted that intragrain plastic deformation near grain boundary triple junction (GBTJ) should be required to accommodate the discontinuity given by grain boundary sliding. The presence of a hard grain having fine oxide particle dispersion near the GBTJ reduces plastic deformation inside the grain, thus suppressing the grain boundary sliding. Too many hard grains, on the other hand, would result in the stress concentration at the GBTJ and deteriorate the creep strength. Therefore, there would be an optimum fraction of residual-α ferrite for reducing grain boundary sliding of the 9Cr-ODS steel. The fraction of residual-α ferrite increases with titanium concentration, since titanium is a strong ferrite-forming element. The optimum amount of residual-α ferrite is considered to be present in 9Cr-ODS steel when the titanium concentration is 0.30–0.35 wt%. The difference in hardness between hard grains and soft grains is also an important factor for improvement of creep strength in the 9Cr-ODS steel. Too large a difference in the hardness should induce the deformation to be concentrated in the soft area, thus deteriorating the creep strength. The inferior creep strength of 35MH to that of 35MS may be traced to a larger difference in hardness between the hard and soft grains of 35MH compared to that of 35MS.

3.4. Tube manufacturing test of high-strength 9Cr-ODS steel

The high strength steel containing 0.30 wt% titanium, 3MS, was sent though the cold pilger-mill process so as to manufacture a thin-walled tube with good creep property. The tube was shown to markedly harden to 380–400Hv by cold-rolling, however, the furnace-cooling permits its hardness to satisfactorily decrease to 340–355Hv in each pass. The cladding tube of 3MS was successfully manufactured with the precise dimensions of 8.5 ± 0.04 mm in diameter $\times 0.5 \pm 0.03$ mm in wall-thickness without any cleavage. It was therefore clarified that the 9Cr-ODS containing 0.30 wt% titanium-3MS has satisfactory workability.

4. Summary

The results of this study can be summarized as follows:

(1) Creep strength of 9Cr-ODS steel can be improved by increasing titanium concentration to 0.3–0.35 wt%. This improvement would be ascribed to an increase of residual-α ferrite containing ultra-fine oxide particles.
(2) The elevation of hot-extrusion temperature from 1150 °C to 1200 °C was shown to increase the fraction of residual-α ferrite, however, it certainly degraded the creep strength of 9Cr-ODS steel. The elevation of hot-extrusion temperature resulted in the softening of tempered martensite area probably due to the coarsening of the oxide particles. This would cause the deterioration of the creep strength.
(3) The 9Cr-ODS steel containing 0.30 wt% titanium – 3MS – was shown to have satisfactory workability and superior creep strength. The cladding tube made of 3MS was successfully manufactured with precise dimensions.

References

[1] A. Kimura, R. Sugano, Y. Matsushita, S. Ukai, J. Phys. Chem. Solids 66 (2005) 504.
[2] S. Ukai, S. Mizuta, M. Fujiwara, T. Okuda, T. Kobayashi, J. Nucl. Sci. Technol. 39 (7) (2002) 778.
[3] S. Ukai, T. Okuda, M. Fujiwara, T. Kobayashi, S. Mizuta, H. Nakashima, J. Nucl. Sci. Technol. 39 (8) (2002) 872.
[4] S. Atamert, J.E. King, Acta. Metall. Mater. 39 (3) (1991) 273.
[5] S. Ohtsuka, S. Ukai, M. Fujiwara, T. Kaito, T. Narita, J. Nucl. Mater. 329–333 (2004) 372.
[6] S. Ohtsuka, S. Ukai, M. Fujiwara, T. Kaito, T. Narita, Mater. Trans. 46 (3) (2005) 487.
[7] M.J. Alinger, G.R. Odette, D.T. Hoelzer, J. Nucl. Mater. 329–333 (2004) 382.
[8] R.L. Klueh, J.P. Shingledecker, R.W. Swindemann, D.T. Hoelzer, J. Nucl. Mater. 341 (2005) 103.
[9] A. Alamo, V. Lambard, X. Averty, M.H. Mathon, J. Nucl. Mater. 329–333 (2004) 333.
[10] R. Lindau, A. Moslang, M. Schirra, P. Schlossmacher, M. Klimenkov, J. Nucl. Mater. 307–311 (2002) 769.
[11] A. Uehira, S. Ukai, T. Mizuno, T. Asaga, E. Yoshida, J. Nucl. Sci. Technol. 37 (9) (2000) 780.
[12] H. Sakasegawa, M. Tamura, S. Ukai, S. Ohtsuka, H. Tanigawa, H. Ogiwara, A. Kohyama, M. Fujiwara, J. Nucl. Mater., submitted for publication.